Virologica Sinica 38 (2023) 585–594

Contents lists available at ScienceDirect

Virologica Sinica

journal homepage: www.keaipublishing.com/en/journals/virologica-sinica
www.virosin.org

Research Article

A high throughput antiviral screening platform for alphaviruses based on Semliki Forest virus expressing eGFP reporter gene

Yu-Jia Shi [a], Jia-Qi Li [b,c], Hong-Qing Zhang [b,c], Cheng-Lin Deng [b,c], Qin-Xuan Zhu [a], Bo Zhang [b,c,*], Xiao-Dan Li [a,*]

[a] Hunan Normal University, School of Medicine, Changsha, 410081, China
[b] Key Laboratory of Special Pathogens and Biosafety, Wuhan Institute of Virology, Center for Biosafety Mega-Science, Chinese Academy of Sciences, Wuhan, 430071, China
[c] University of Chinese Academy of Sciences, Beijing, 100049, China

ARTICLE INFO

Keywords:
Alphavirus
Semliki Forest virus
Reporter virus
High throughput screening
Inhibitor

ABSTRACT

Alphaviruses, which contain a variety of mosquito-borne pathogens, are important pathogens of emerging/re-emerging infectious diseases and potential biological weapons. Currently, no specific antiviral drugs are available for the treatment of alphaviruses infection. For most highly pathogenic alphaviruses are classified as risk group-3 agents, the requirement of biosafety level 3 (BSL-3) facilities limits the live virus-based antiviral study. To facilitate the antiviral development of alphaviruses, we developed a high throughput screening (HTS) platform based on a recombinant Semliki Forest virus (SFV) which can be manipulated in BSL-2 laboratory. Using the reverse genetics approach, the recombinant SFV and SFV reporter virus expressing eGFP (SFV-eGFP) were successfully rescued. The SFV-eGFP reporter virus exhibited robust eGFP expression and remained relatively stable after four passages in BHK-21 cells. Using a broad-spectrum alphavirus inhibitor ribavirin, we demonstrated that the SFV-eGFP can be used as an effective tool for antiviral study. The SFV-eGFP reporter virus-based HTS assay in a 96-well format was then established and optimized with a robust Z′ score. A section of reference compounds that inhibit highly pathogenic alphaviruses were used to validate that the SFV-eGFP reporter virus-based HTS assay enables rapid screening of potent broad-spectrum inhibitors of alphaviruses. This assay provides a safe and convenient platform for antiviral study of alphaviruses.

1. Introduction

Alphaviruses which belong to the family *Togaviridae*, comprise a group of mosquito-borne viruses that cause severe disease to humans and animals. Based on the originated geography and disease progression, alphaviruses are divided into the New World and Old World groups. The New World viruses include Venezuelan equine encephalitis virus (VEEV), eastern equine encephalitis virus (EEEV) and western equine encephalitis virus (WEEV) which cause fatal encephalitis to humans, while the Old World viruses such as Chikungunya virus (CHIKV), Mayaro virus (MAYV), Ross River virus (RRV), Sindbis virus (SINV) and Semliki Forest virus (SFV) are often associated with arthritogenic diseases. Due to the wide distribution of the mosquito vectors, alphaviruses have become the important cause of emerging and re-emerging infectious diseases. The recent examples are the continuing CHIKV epidemics in India since 2005 and the outbreaks of MAYV in tropical regions of South American countries (Azar et al., 2020). The VEEV, EEEV and WEEV cause incapacitating or fatal infections in humans and horses, Although their outbreaks were often sporadic, there is possibility that these viruses could be transmitted by aerosols, making them potential bioterror agents (Roy et al., 2010). Currently, there are no specific antivirals for the treatment of human alphavirus infection. A significant challenge for antiviral research on alphaviruses is that most pathogenic alphaviruses are classified into risk group-3 pathogens (CHIKV, MAYV, VEEV, EEEV, WEEV, etc.), and the containment requirements of BSL-3 laboratory for live virus manipulation hinders the antiviral development of these viruses.

The genome of alphaviruses is a positive single stranded RNA containing two open reading frames (ORFs) flanked by untranslated regions (UTR) with a 5′ cap and a 3′ poly(A) tail. The 5′ ORF encodes the nonstructural proteins (nsP1–nsP4) which form viral replication complex (RC) that is responsible for viral genome replication and transcription of the subgenomic RNA (sgRNA). The 3′ ORF is translated from the sgRNA

* Corresponding authors.
E-mail addresses: zhangbo@wh.iov.cn (B. Zhang), lxd@live.cn (X.-D. Li).

https://doi.org/10.1016/j.virs.2023.06.007
Received 3 February 2023; Accepted 20 June 2023
Available online 28 June 2023

and encodes viral structural proteins (capsid, E3, E2, 6K and E1). The viral nonstructural proteins of different alphaviruses have similar functions and enzymatic activities (Reichert et al., 2009). For example, the structure of nsP2, which possesses helicase, RNA triphosphatase and protease activities that are essential for viral replication, is conserved among the New and Old World alphaviruses (Shin et al., 2012). Crystal structure study also identified that RNA-dependent RNA polymerase (RdRp) domain of nsP4 of RRV and SINV have similar structure. Recent studies have demonstrated that the replication complex of alphaviruses of SFV groups can cross-utilize RNA templates of heterologous alphaviruses (Lello et al., 2020), and SFV tolerates substitution of nsP2 and nsP3 domains with those of CHIKV (Teppor et al., 2021). These findings indicate that the replicase proteins of alphaviruses have common mechanisms in modulating viral replication. Furthermore, a recent study demonstrated that multiple alphaviruses including SFV, EEEV, and SINV share the same receptors in vertebrate cells (Clark et al., 2022). These common features of the viral proteins of different alphaviruses make them potential targets for screening pan-alphavirus antivirals that inhibit viral replication and infection. Therefore, for highly pathogenic alphaviruses, the antiviral screening could be performed using the less pathogenic alphaviruses which can be manipulated under BSL-2 condition as an alternative.

SFV infection causes self-limited febrile diseases in humans including fever, headache, and arthralgia, and most infections are asymptomatic or very mild. However, in mice, SFV is able to enter the central nervous system (CNS) and infect neurons and oligodendrocytes, leading fatal diseases to the animals (Fazakerley, 2002). The features of relatively low level of virulence in humans, high neuroinvasion in mice, and ability to be handled in BSL-2 laboratory, make SFV a good model to investigate the mechanisms of viral replication and pathogenesis, and to conduct antiviral screening for alphaviruses. In fact, several compounds showing inhibitory effect to CHIKV or VEEV such as ribavirin (Rothan et al., 2015), IFN-α/β (Briolant et al., 2004), 3′-fluoro-3′-deoxyadenosine (Smee et al., 1992) and chloroquine (Khan et al., 2010) were first found to have antiviral effect to SFV (Huffman et al., 1973; Maheshwari et al., 1983; Van Aerschot et al., 1989; Perez et al., 1993), confirming the application of SFV as a surrogate in antiviral screening for inhibitors against the highly pathogenic alphaviruses in BSL-2 facilities.

The development of reverse genetics system allows the insertion of a reporter gene into viral genome to generate reporter virus, whose replication can be easily monitored by the expression of reporter genes. The reporter virus provides an efficient platform for high-throughput antiviral screening (HTS) of antivirals targeting to the entire viral life cycle. Currently, the reverse genetics system and reporter virus had been established in many viruses including several flaviviruses (Zou et al., 2011; ZR Zhang et al., 2020a; Zhang et al., 2021), coronaviruses (Xie et al., 2020; Amarilla et al., 2021), influenza viruses (Weisshaar et al., 2016; Creanga et al., 2021) and alphaviruses (Liljestrom et al., 1991; Tarbatt et al., 1997; Tamberg et al., 2007; Pohjala et al., 2008; Deng et al., 2016; Li et al., 2019). In these systems, the fluorescent and luminescent protein genes are the most commonly used genes for reporter virus construction. The luciferase readouts are quantitative with low background both *in vitro* and *in vivo*, but require addition of the corresponding chemical substrates, such as *Renilla* luciferase, which requires the lysis of cells prior to detection. Fluorescent proteins are preferred in cell-based antiviral screening due to their direct visualization in living cells without substrates or cell lysis, and thus are amenable to provide dynamic monitoring during the experiments. The results of fluorescent proteins are qualitative when examined under traditional fluorescence microscopy. However, with the development of high content screening (HCS) system which combines the cellular imaging and high-throughput techniques, parameters such as number, intensity and distribution of the fluorescent proteins can be quantitatively acquired. Therefore, using the HCS instrument, the fluorescent proteins exploit the advantages of both direct visualization and quantification, making them ideal choice as the reporters of viruses in cell-based HTS for antiviral study.

In this study, to circumvent the requirement for BSL-3 facilities when working with the live highly pathogenic alphaviruses in drug discovery, we developed a high-throughput antiviral assay based on an eGFP-tagged SFV reporter virus (SFV-eGFP) as a useful alternative. SFV-eGFP was generated using reverse genetic approach. It showed comparable replication to the wild type SFV, and the expression of eGFP could represent the virus propagation. Based on the live cell imaging by HCS system, SFV-eGFP was applied to establish an HTS antiviral platform in 96-well format. Using the known alphavirus inhibitors, we demonstrated that SFV-eGFP can serve as a surrogate that can be performed in BSL-2 laboratories to facilitate the antiviral development of pathogenic alphaviruses.

2. Materials and methods

2.1. Cells, viruses and antibodies

Baby hamster kidney-21 (BHK-21) (ATCC CCL-10), Vero (ATCC CCL-81), Hela (ATCC CCL-2), and Huh-7 (CVCL_0336) cells were cultured in Dulbecco's modified Eagle's medium (DMEM) (11965092, Gibco, US) supplemented with 10% fetal bovine serum (FBS) (16140071, Gibco, US), 100 units/mL of penicillin and 100 μg/mL of streptomycin, and maintained in 5% CO_2 at 37 °C. The parental SFV4 virus stock (GenBank: KP699763.1) was kindly provided by Professor Xi Zhou from Wuhan Institute of Virology, CAS, and the virus stocks were propagated in BHK-21 cells. The recombinant SFV and SFV-eGFP were rescued by transfection of BHK-21 cells with *in vitro* transcribed RNAs from the SFV and SFV-eGFP infectious clones (described below) respectively. The CHIKV E2 polyclonal antibody which was generated by immunization of BALB/c mice with SDS-PAGE purified CHIKV E2 protein, had cross-reactivity with SFV virus, and was used to detect the expression of SFV E2 protein. FITC-conjugated goat anti-mouse IgG, and Alexa Fluor 568 conjugated goat anti-mouse IgG which were used as secondary antibodies were purchased from Protein Tech Group Inc. (Cat No. SA00003-1, US) and Thermo Fisher Scientific (A-11031, US).

2.2. Plasmid construction

For the construction of SFV (GenBank: KP699763.1) infectious clone, the SFV viral RNA was extracted from 140 μL parental virus stock using QIAamp Viral RNA Mini Kit (Qiagen, Germany) according to the standard procedures. RT-PCR assay was performed using the SFV viral RNA as template to amplify three fragments covering the full-length genome of SFV4 which contained the nucleotides from 1 to 3058 (fragment A), 3035 to 7384 (fragment B), and 7419 to 11474 (fragment C), respectively. The sequences of the primers used for amplifying the fragments were listed in Supplementary Table S1. Fragment A had an *Afe*I restriction site and a SP6 promoter upstream the 5′UTR of SFV, and fragment B contained an *Asc*I and a *Not*I restriction site at the 3′ terminal. Fragment A and B were fused through overlap PCR, and cloned into a modified pACYC vector at the *Afe*I and *Not*I restriction sites, generating the plasmid pACYC-SFV-A + B. Fragment C were amplified and inserted into pACYC-SFV-A + B at *Asc*I and *Not*I sites. The resulting plasmid containing the full-length genome of SFV4 was named as pACYC-SFV (Fig. 1A).

To generate the SFV-eGFP infectious clone, the fragment containing the 6601–7401 nt sequence, the *eGFP* gene and an additional subgenomic promoter sequence (5′-GTTATACACCTCTACGGCGGTCCTAGATTGGTG CGTTAA-3′) was generated by two rounds of overlap PCR. Briefly, the fragments "6601–7401 nt" and "2ndsg promoter-*Asc*I-Capsid" were amplified using pACYC-SFV as template, and the *eGFP* gene was amplified using pEGFPN1 plasmid as template. The *eGFP* gene and "2ndsg promoter-*Asc*I-Capsid" were first fused together by first round of overlap PCR, and the resulting product "eGFP-2ndsg promoter-*Asc*I-Capsid" were then fused with "6601–7401 nt" sequence by the second step overlap PCR. The final fragment "6601–7401 nt-eGFP-2ndsg promoter-*Asc*I-Capsid" was inserted into pACYC-SFV with *Xba*I and *Asc*I restriction sites.

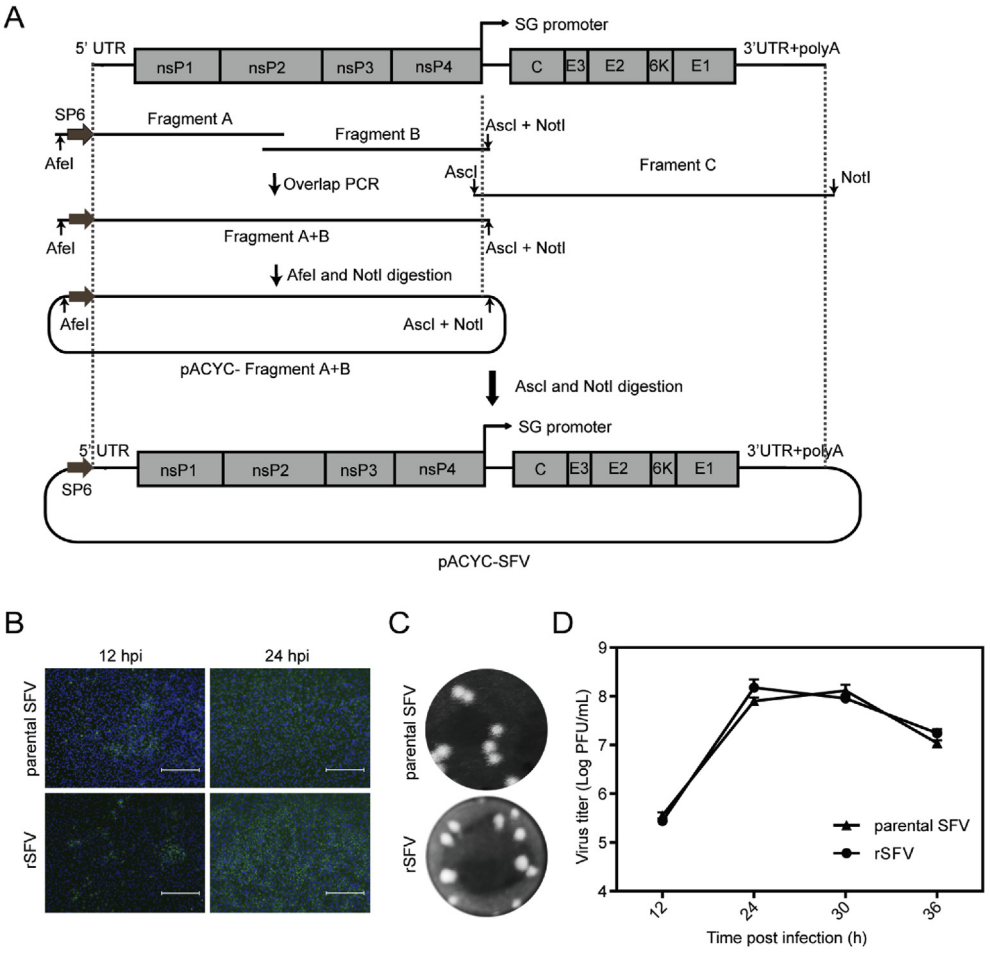

Fig. 1. Construction and characterization of a recombinant SFV. **A** Schematic representation of the strategy to construct the infectious clone of SFV4 strain. The detailed information of the construction and assembly of sub-genomic clones was described in Materials and methods. **B** The E2 protein expression in the parental and recombinant SFV infected cells. The recombinant SFV was rescued by transfection of the RNA transcribed from the pACYC-SFV infectious clone into BHK-21 cells, and the supernatant was harvested at 48 h post transfection. BHK-21 cells were infected with the parental SFV or recombinant SFV (rSFV) at an MOI of 0.1, and the cells were fixed and subjected to IFA assay using the polyclonal antibody against CHIKV E2 which is cross-reactive to SFV E2 protein as the primary antibody and FITC-conjugated goat anti-mouse IgG as secondary antibody at the indicated time points. The nuclei were stained with DAPI. Scale bars represent 300 μm. **C** The plaque morphology of the parental SFV and rSFV determined by single-layer plaque assay. **D** Comparison of the growth kinetics of parental SFV and rSFV. BHK-21 cells were infected with parental SFV or rSFV at an MOI of 0.1, and the supernatants were harvested at the indicated time points and subjected to plaque assay to determine the viral titers. Error bars indicate the standard deviations from three independent experiments.

The infectious clone of SFV-eGFP reporter virus was designated as pACYC-SFV-eGFP. The sequences of the primers used for amplifying the fragments were listed in Supplementary Table S1. All constructs were confirmed by sequencing before use.

2.3. RNA transcription and transfection

The infectious clones were linearized by *Spe*I and purified by phenol/chloroform extraction. The SFV and SFV-eGFP RNAs were transcribed from the corresponding linearized plasmids using SP6 mMEGAscript® Kit (Invitrogen, US) according to the manufacturer's protocols. Approximately 1 μg RNA was transfected into BHK-21 cells with DMRIE-C (Invitrogen, US) reagent. Supernatants of the transfected cells were collected at different time points after transfection, and the virus was aliquoted and stored at −80 °C for use in all experiments.

2.4. Immunofluorescence assay (IFA) and plaque assay

The RNA transfected cells were seeded on a Chamber Slide (ThermoFisher). At different time points after transfection, the cells were fixed with cold (−20 °C) 5% acetic acid in methanol for 10 min at room temperature, washed three times with PBS and then incubated with mouse polyclonal antibody against CHIKV E2 (1:300 dilution with PBS) for 1 h. After washing with PBS three times, the cells were incubated with goat anti-mouse IgG conjugated with Alexa Fluor 568 (A-11031, ThermoFisher, US) (1:1000 dilution with PBS) at room temperature for 1 h. Following three times of PBS washing, the slides were mounted with 95% glycerol and analyzed under a fluorescence microscope (Nikon Eclipse TE2000, NIKON, Japan) at 400× magnification. Virus titer and morphology were determined by single layer plaque assay with standard procedure as described previously (Deng et al., 2016).

2.5. Reverse transcription PCR assay

To test the stability of the SFV-eGFP, the reporter virus was serially passaged in BHK-21 cells for six rounds. For each passage, the supernatants were collected and total RNAs of the infected cells were extracted using Trizol reagent (TAKARA, Japan). Viral RNAs of each passage were amplified by one-step RT-PCR using a PrimeScript RT-PCR kit (TAKARA, Japan) with primers spanning nsP4 to capsid gene (forward primer: 5′-

GACCGCCTGCCGTGTTTC-3′ and reverse primer: 5′-GACTTCGAAGATACAGTC-3′). The amplified products were analyzed by electrophoresis on 1% agarose gel.

2.6. Viral growth kinetics

Growth kinetics of SFV and SFV-eGFP viruses on BHK-21 were examined. Approximately 2.5×10^5 BHK-21 cells were seeded in a 35 mm dish. After incubation overnight, the cells were infected with 400 μL SFV or SFV-eGFP virus at MOIs of 0.1. After incubation for 2 h, the supernatants were collected and the cells were washed with PBS for three times and replaced with fresh medium with 2% FBS. At different time points after infection, the culture medium was collected and stored at −80 °C, and subsequently subjected to plaque assay to determine the viral titer. For SFV-eGFP infection, the expression of *eGFP* gene was observed under the fluorescence microscope (Nikon Eclipse TE2000, NIKON) at 100× magnification.

2.7. Antiviral assay of SFV-eGFP

BHK-21 cells were seeded into 24-well plates at a density of 8×10^4 cells per well. Twenty-four hours later, the cells were infected with SFV or SFV-eGFP at an MOI of 0.1 and incubated with various concentrations of ribavirin (0 μmol/L–82 μmol/L). For each drug concentration, two wells were performed in parallel. After incubation at 37 °C for 24 h, the supernatants were collected and viral titers were quantified by plaque assay. For SFV-eGFP infection, the expression of *eGFP* gene was observed under the fluorescence microscope (Nikon Eclipse TE2000, NIKON) at 100× magnification.

2.8. Optimization and verification of the SFV-eGFP based HTS assay

The SFV-eGFP based HTP screening assay was developed in a 96-well plate format using ribavirin as the positive drug. BHK-21 cells were seeded into 96-well plates at a density of 0.5, 1 and 2×10^4 cells per well respectively, and cultured for 24 h at 37 °C. The cells were infected with SFV-eGFP at varying MOIs of 0.01, 0.1 or 1, and incubated with various concentrations of ribavirin (0 μmol/L–82 μmol/L). For each condition, six wells were performed in parallel. At 24 h post-infection (hpi) and 36 hpi, the number of eGFP positive cells and fluorescence intensity were detected by a PerkinElmer HCS system (ZR Zhang et al., 2020b). To evaluate the performance of the HTS assay, the signal-to-noise ratio (S/N) and Z′ factor values were calculated. S/N was calculated as S/N = (mean of negative control − mean of positive control)/standard deviation (SD) of positive control. The Z′ value was calculated as $Z' = 1 - (3 \times$ SD of positive control + 3 × SD of negative control)/|mean of positive control − mean of negative control|. The Z′ factor between 0.5 and 1 indicates an excellent assay with good separation between controls (Zhang et al., 1999).

The known inhibitors of pathogenic alphaviruses including oxysophoridine, gemcitabine, sorafenib, dasatinib and chlorhexidine HCl (CHL) were used to verify whether the SFV-eGFP based HTS assay can be used to screen broad-spectrum antivirals against alphaviruses. Rapamycin which had no inhibitory effect on alphavirus was used as negative drug. BHK-21 cells were seeded into 96-well plates at a density of 1×10^4 cells per well and cultured for 24 h at 37 °C. Twenty-four hours later, the cells were infected with SFV-eGFP at an MOI of 1, and incubated with the above compounds at a reference concentration. At 24 hpi, the number of eGFP positive cells and fluorescence intensity were detected by the HCT screening system. For each kind of drug, six wells were performed in parallel.

The concentration for 50% of maximal effect (EC_{50}) of each compound were determined by the eGFP signal detected by HTS assay and viral titers detected by plaque assay, respectively. BHK-21 cells were seeded into 96-well plates at a density of 1×10^4 cells per well. Twenty-four hours later, the cells were infected with SFV-eGFP at an MOI of 1 and incubated with various concentrations of gemcitabin, CHL, dasatinib, oxysophoridine, and sorafenib, respectively. For each drug concentration, three wells were performed in parallel. After incubation at 37 °C for 24 h, the number of eGFP positive cells was detected by the HCS system, and the supernatants were collected and viral titers were quantified by plaque assay.

2.9. Cytotoxicity assay

BHK-21 cells were seeded into 96-well plates at a density of 1×10^4 cells per well and cultured for 24 h at 37 °C. Then, serial 2-fold dilutions of gemcitabin, CHL, dasatinib, oxysophoridine and sorafenib were added to the cells, respectively. After 48 h, the cells were incubated with 10 μL CCK-8 reagent (cell counting kit-8, Bimake, US) for 1 h at 37 °C. The absorbance at 450 nm was read by a Microplate Reader (Varioskan Flash, Thermo Fisher). Cell viability was expressed as a percentage of the treated cells to the DMSO treated control cells. For each compound concentration, six wells were performed in parallel, and the mean values of the cell viability were calculated.

2.10. Statistical analysis

GraphPad Prism software was used to analyze the data. All the values were exhibited as mean ± standard deviation (SD). The EC_{50} values were calculated by nonlinear regression to determine the drug concentration required to achieve 50% of viral titer reduction or fluorescence value reduction. The 50% cytotoxic concentration (CC_{50}) values were calculated by nonlinear regression analysis to measure the cytotoxic concentration required to achieve 50% of the cell viability. The differences between the compound treated groups and control group were analyzed using one-way ANOVA.

3. Results

3.1. Development of an infectious clone of SFV4 strain

In order to establish the reverse genetics system of SFV, we first constructed an infectious clone of the SFV4 strain, which has been engineered to a mature viral vector for gene therapy and vaccine design (Lundstrom, 2014, 2020). As depicted in Fig. 1A, using the SFV viral RNA as template for RT-PCR assay, three fragments covering the full-length genome sequence were obtained. The fragment A contained a bacteriophage SP6 promoter and 1–3058 nt sequence of SFV genome, fragment B included the 3035–7384 nt sequence, and fragment C covered the 7419–11474 nt sequence and a poly(A) tail with 26 adenosines. The fragments A and B were fused by overlap PCR and cloned into a low-copy-number vector pACYC177, and then fragment C was inserted into this intermediate subclone. The resulting infectious clone covering the full-length genome of SFV4 was named as pACYC-SFV. The RNA transcribed from pACYC-SFV was transfected into BHK-21 cells. The cytopathic effect of the transfected cells appeared at 24 h post-transfection (hpt), and massive cell death was observed at 36 hpt, suggesting that the recombinant SFV (rSFV) was successfully rescued by the infectious clone. To compare the replication of the rSFV and the parental SFV virus, BHK-21 cells were infected with rSFV or parental SFV with an MOI of 0.01, and the viral protein expression, the growth curve and plaque morphology were determined by IFA and plaque assays, respectively. As shown in Fig. 1B, in both rSFV and parental SFV infected cells, clustered IFA-positive cells were observed at 12 hpi, and the cells were 100% positive at 24 hpi. The rSFV and parental SFV showed similar plaque morphology and growth kinetics with the peak viral titer of 1.6×10^8 PFU/mL and 2×10^8 PFU/mL respectively (Fig. 1C and D), indicating that the rescued rSFV had comparable replication level with the parental SFV virus.

3.2. Production of the SFV-eGFP reporter virus

Using a double-subgenomic strategy employed by several alphavirus reporter viruses (Deng et al., 2016; Li et al., 2019), we generated the infectious SFV that includes *eGFP* reporter gene. As shown in Fig. 2A, the pACYC-SFV infectious clone was used as backbone, the *eGFP* gene with an additional subgenomic promoter was inserted downstream the original subgenomic promoter of SFV genome, generating the infectious clone of pACYC-SFV-eGFP. The *in vitro* transcribed SFV-eGFP RNAs were transfected into BHK-21 cells to rescue the reporter virus. As seen in Fig. 2B, the number of eGFP-positive cells dramatically increased from 12 hpt to 96 hpt, suggesting the successful rescue of the reporter virus. The expression of SFV E2 protein was simultaneously detected by IFA. It was found that the cells expressing SFV E2 were also eGFP positive, indicating that the eGFP expression can represent viral replication of SFV-eGFP. Then, we compared the replication of SFV-eGFP and the wild type SFV. BHK-21 cells were infected with SFV-eGFP and SFV at an MOI of 0.1 respectively, and viral titers at different time points after infection were determined by plaque assay. During infection, SFV produced faster cytopathic effect CPE than SFV-eGFP (Fig. 2C). Progressive CPE were observed in the SFV and SFV-eGFP infected cells since 24 hpi and 36 hpi, respectively. We found that SFV-eGFP exhibited a smaller plaque morphology (Fig. 2D) and slower kinetics than that of wild type SFV (Fig. 2E). However, the peak SFV-eGFP titer reached 10^7 PFU/mL at 48 hpi, indicating the ability to produce this virus with high titer.

3.3. The genetic stability of SFV-eGFP in vitro

We next tested the genetic stability of *eGFP* gene in SFV-eGFP infected cells. Different cell types including BHK-21, Vero, Huh7, and Hela cells were infected with SFV-eGFP P0 viruses at MOIs of 0.01, 0.1 and 1, respectively, and the eGFP expression was observed at different time points after infection. We found that in BHK-21, the numbers of eGFP positive cells correlated well with the dose of viral infection and increased over time that almost 100% of the infected cells were eGFP positive at 36 hpi. However, in Vero and Huh7 cells, there was no significant increase of the eGFP expression from 24 hpi to 36 hpi, but obvious CPE was observed at 48 hpi (data not shown), suggesting that the *eGFP* gene was removed from the SFV-eGFP genome in these cells. In Hela cells, only sporadic eGFP positive cells were detected during the infection, indicating that the virus cannot propagate in Hela cells (Fig. 3). Therefore, BHK-21 cells were used for serially blind passage of SFV-eGFP for six rounds to further examine the *eGFP* gene stability (Fig. 4A). At each passage, the viruses were harvested when robust CPE was observed. The eGFP expression was analyzed, and the total cellular RNAs were extracted from the infected cells. As shown in Fig. 4B, at P1 to P4, nearly 100% of the infected cells expressed high levels of eGFP, while reduced eGFP expression was observed in P5 and P6 infected cells, suggesting the significant loss of eGFP beginning from passage 4. The P1 to P6 RNAs were subjected to RT-PCR assay to amplify the fragment spanning from nsP4 to capsid genes. The expected products for SFV-eGFP and wild type SFV are about 1.5 kb and 0.7 kb respectively. The result showed that although weaker bands of different smaller lengths were exhibited from P2 to P4 RNAs, the 1.5 kb band was still predominant in P1–P4 templates, whereas the smaller bands were increasingly apparent in P5 and P6 RNAs, confirming that SFV-eGFP is relatively stable within four rounds of passages, but was significantly lost since P5 (Fig. 4C). However, it is able to prepare the virus stocks that retained high levels of eGFP expression within three passages.

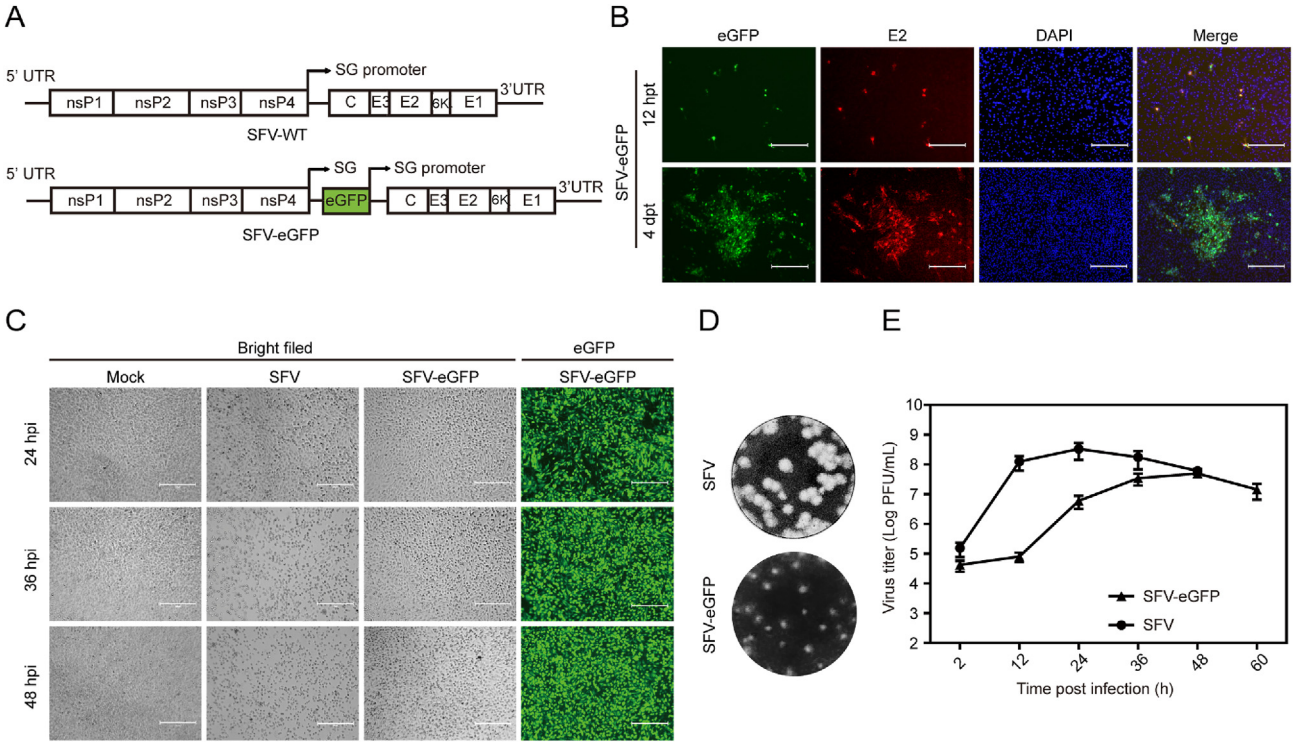

Fig. 2. Characterization of the SFV-eGFP reporter virus. **A** Sketch of the SFV-eGFP reporter virus genome. The *eGFP* gene (shown in the green box) with an additional subgenomic promoter was inserted between the two ORFs of the SFV genome. **B** The expression of viral E2 protein and eGFP in the SFV-eGFP RNA transfected cells. About 1 μg SFV-eGFP RNA which was *in vitro* transcribed from the SFV-eGFP infectious clone was transfected into BHK-21 cells. At the indicated time points after transfection, the cells were fixed with 4% paraformaldehyde, and the eGFP signal was detected under the fluorescence microscope, the expression of viral E2 protein was analyzed by IFA using the polyclonal antibody against CHIKV E2 as the primary antibody and Alexa Fluor 568 conjugated goat anti-mouse IgG as secondary antibody. The nuclei were stained with DAPI. Scale bars represent 300 μm. **C** The bright filed and fluorescence images of the SFV-eGFP and SFV infected BHK-21 cells at the indicated time points after infection. Scale bars represent 300 μm. **D** The plaque morphology of SFV and SFV-eGFP viruses determined by single-layer plaque assay. **E** The growth kinetics of the SFV and SFV-eGFP viruses on BHK-21 cells at an MOI of 0.1. Error bars indicate the standard deviations from three independent experiments.

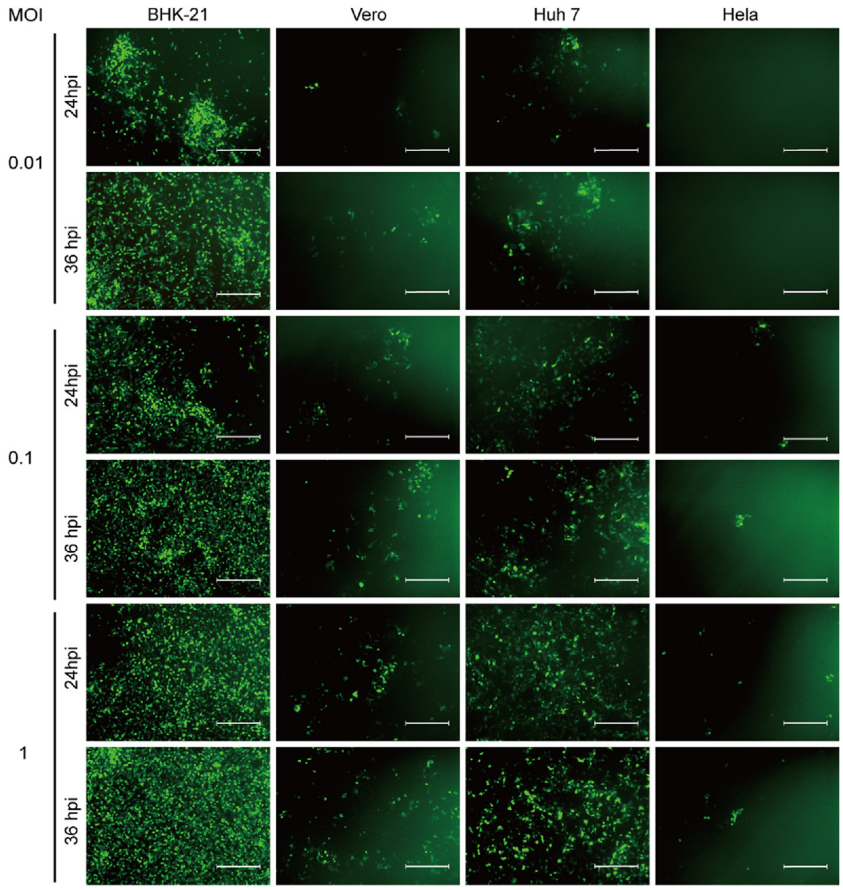

Fig. 3. Growth of SFV-eGFP reporter virus in different cell types. BHK-21, Vero, Huh 7, and Hela cells were infected with SFV-eGFP P0 virus which was harvested from the SFV-eGFP RNA transfected BHK-21 cells at MOIs of 0.01, 0.1 and 1, respectively. The eGFP expression was detected at the indicated time points after infection under the fluorescence microscope. Scale bars represent 300 μm.

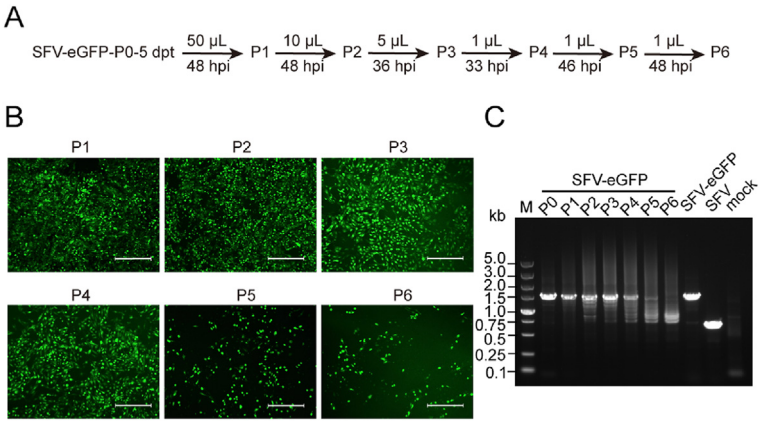

Fig. 4. The genetic stability of SFV-eGFP reporter virus on BHK-21 cells. **A** The flow chart of the serial passage of SFV-eGFP in BHK-21 cells. **B** The expression of eGFP in the BHK-21 cells infected with each passage virus. Scale bars represent 300 μm. **C** RT-PCR analysis of the RNAs extracted from cells infected with each passage virus using primers spanning from *nsP4* to *capsid* gene. The *in vitro* transcribed wild type SFV and SFV-eGFP RNAs were used as controls to distinguish the bands. The total RNAs extracted from uninfected BHK-21 cells (mock) were used as negative control. The RT-PCR products were visualized by 1% agarose gel electrophoresis.

3.4. The SFV-eGFP virus-based antiviral assay

We generated SFV-eGFP P0 virus stocks to assess the utility of the reporter virus for antiviral analysis. The inhibitory effects of the known inhibitor ribavirin on SFV-eGFP and wild type SFV were tested *in vitro*. BHK-21 cells were infected with SFV-eGFP or SFV with MOI of 0.1, and treated with a range of concentrations of ribavirin respectively. At 24 hpi, the eGFP expression was detected, and the viral titers of the supernatants of the cells were determined by plaque assay. As shown in Fig. 5A and B, ribavirin efficiently inhibited the growth of SFV-eGFP in a dose-dependent manner that both the number of eGFP-positive cells and viral titer reduced with the increase of the drug concentration. The EC_{50}

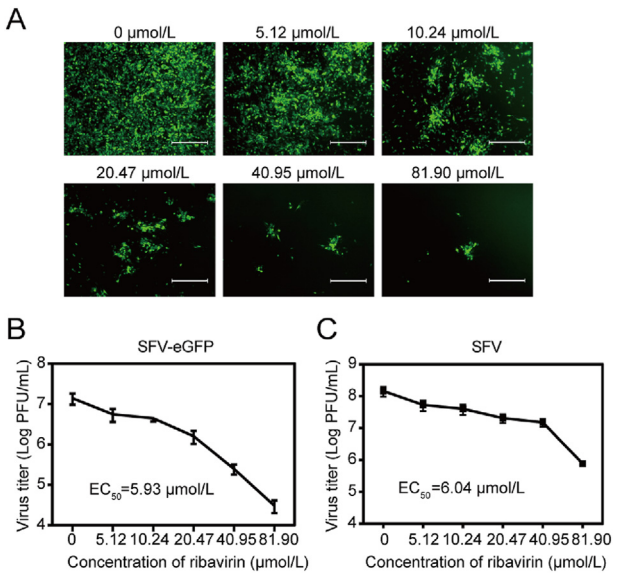

Fig. 5. The SFV-eGFP can be used as a tool for antiviral testing. **A** The effect of different concentrations of ribavirin on the expression of eGFP in SFV-eGFP infected cells. BHK-21 cells were infected with SFV-eGFP (MOI = 0.1), and incubated with medium containing the indicated concentrations of ribavirin. The eGFP expression was detected at 24 hpi. Scale bars represent 300 μm. The inhibitory effect of ribavirin on viral titer of SFV-eGFP (**B**) and wild type SFV (**C**). BHK-21 cells were infected with SFV-eGFP or SFV at an MOI of 0.1, respectively, and treated with the indicated concentrations of ribavirin. The supernatants of the cells were collected at 24 hpi and subjected to plaque assay to determine the viral titers. Error bars indicate the standard deviations from three independent experiments.

values measured by virus titers for SFV-eGFP and wild type SFV were 6.04 μmol/L and 5.93 μmol/L (Fig. 5C), respectively. These results confirmed that SFV-eGFP can be applied for antiviral screening, and that the antiviral activity can be rapidly evaluated by the eGFP expression reduction in the infected cells.

3.5. Optimization for HCS using SFV-eGFP virus

To develop a suitable condition for the SFV-eGFP virus-based HTS assay, the parameters including virus MOI, cell density, and incubation time were optimized. Different numbers of BHK-21 cells (5000, 10,000 and 20,000 cells per well) were seeded in a 96-well format. After 24 h, the cells were infected with SFV-eGFP P0 virus with MOIs of 0.01, 0.1 and 1, respectively. To validate the effectiveness of each condition, the infected cells were treated with 41 μmol/L ribavirin or PBS control. The numbers of eGFP-positive cells were determined by a HCS system at 24 and 36 hpi, respectively. The Z′ factor which represents the quality of HTS assay (Zhang et al., 1999) was calculated according to the differentiation of the eGFP signal of the ribavirin and PBS treated cells. In a reliable HTS assay, Z′ factor is preferred to be between 1 and 0.5 (Zhang et al., 1999). We found that the cell density and the MOI of virus had significant effects on Z′ factor. As shown in Fig. 6, although ribavirin exhibited >90% inhibitory efficiency under all conditions, fewer cell numbers and amount of virus couldn't achieve robust eGFP signals and resulted in low Z′ values. When the cell density was more than 10,000 cells per well, and the virus MOI was 1, the Z′ values were higher than 0.6 at both 24 hpi and 36 hpi. Considering that the virus infection induced strong CPE at 36 hpi which may interfere with the quantifiable target cell numbers, the optimal conditions amenable to HTS assay were determined to be 10,000 cells/well, MOI of 1, and 24 h of incubation. A Z′ factor of 0.78, and a high signal-to-noise ratio (S/N) of 173.97 were calculated under this condition.

3.6. Validation of the availability of SFV-eGFP virus-based HCS assay for identifying antiviral agents against alphaviruses using reference compounds

To confirm that the established SFV-eGFP reporter virus-based HTS assay can be used to identify antiviral drugs against highly pathogenic alphaviruses, we evaluated the effects of a panel of reference compounds which have been demonstrated to inhibit different alphaviruses on SFV-eGFP under the optimized HTS conditions. Oxysophoridine and gemcitabine are broad-spectrum antiviral compounds whose antiviral activity against SARS-CoV-2 and CHIKV has been identified in our previous studies (YN Zhang et al., 2020) and unpublished work. Sorafenib has been published as an inhibitor of several alphaviruses including VEEV, EEEV, CHIKV and SINV (Lundberg et al., 2018). Dasatinib, known as a tyrosine kinase inhibitor for the treatment of certain types of leukemia (Steinberg, 2007), and Chlorhexidine HCl (CHL) which is used as a disinfectant and has potential antiviral effect (Huang and Huang, 2021), have been proved to have antiviral activity against CHIKV in our work (unpublished data). Rapamycin, that alphaviruses were insensitive (Mohankumar et al., 2011; Joubert et al., 2015), was used as a negative control, and ribavirin was set as positive control. As shown in Fig. 7, the eGFP signals were significantly inhibited by oxysophoridine, gemcitabine, sorafenib, dasatinib, CHL and ribavirin, whereas rapamycin treatment exhibited comparable eGFP-positive cells with the DMSO control. The Z′ factor of this assay was 0.55.

To further demonstrate the effectiveness of the SFV-eGFP based HTS assay, we evaluated the EC_{50} of gemcitabine, sorafenib, oxysophoridine, dasatinib and CHL using the plaque reduction assay and the HTS assay. The SFV-eGFP infected cells in 96-well plates were treated with various concentration of each compound, and the eGFP expression levels and viral titers were determined by HTS assay and plaque assay, respectively. As shown in Fig. 8, all of the compounds inhibited the eGFP signals and viral titers in a dose-dependent manner, and the results showed that there is good correlation between the HTS assay and plaque assay (Supplementary Figs. S1A–S1E). For each compound, the EC_{50} value calculated by reduction of viral titers was lower than that calculated by reduction of eGFP signals, but linear regression analysis showed strong correlation between the two calculations (Supplementary Fig. S1F), suggesting that the HTS assay had similar sensitivity as plaque assay. Furthermore, we had tested the cytotoxicity of these compounds on BHK-21 cells using CCK-8 assay (Supplementary Fig. S2). The CC_{50} values of the five compounds were 3–88 times higher than the EC_{50} values calculated by viral titers, suggesting that these compounds exhibit true antiviral effect but no cytotoxic effect to the cells under the EC_{50} concentrations. These data demonstrated that the compounds that inhibit highly pathogenic alphaviruses are also effective in suppressing the replication of SFV-eGFP.

Overall, these results suggest that SFV-eGFP is a useful surrogate for antiviral screening for agents against highly pathogenic alphaviruses, and the SFV-eGFP reporter virus-based HCS assay provides an efficient platform for rapid antiviral drug discovery.

4. Discussion

Alphaviruses contain many zoonotic pathogens threatening the health of human and livestock worldwide. At present, there is no approved antiviral drug for the treatment of alphaviruses infection. Since most of the pathogenic alphaviruses such as VEEV, EEEV and CHIKV are classified as BSL-3 restricted viruses, the requirement for high biosafety greatly limits their antiviral development. In this study, using reverse genetics method, we constructed a SFV reporter virus expressing eGFP (SFV-eGFP) as a safe surrogate for highly pathogenic alphaviruses in antiviral study without the requirement for BSL-3 facility. After corroborating the ability to yield high titers and the relative genetic stability of the SFV-eGFP reporter virus, the virus was adapted to a robust image-based HTS antiviral assay that enabled rapid identification of potent broad-spectrum inhibitors of alphaviruses.

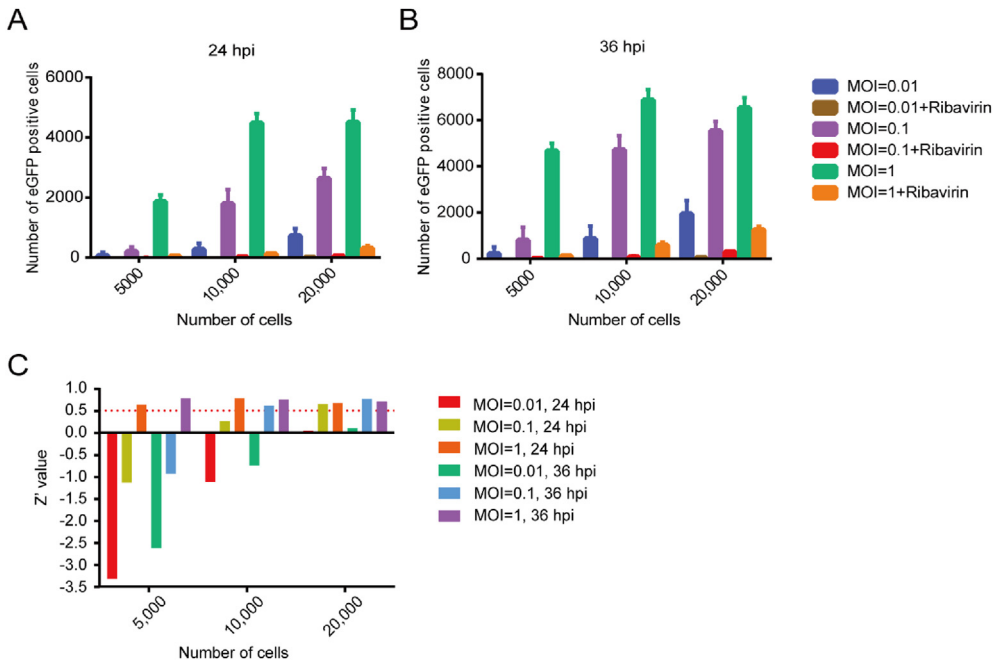

Fig. 6. The optimization of SFV-eGFP based high throughput screening assay parameter. Different numbers of BHK-21 cells were seeded in 96-well plates, and were infected with various MOIs (0.01, 0.1, and 1) after 24 h. The infected cells were treated or untreated with 41 μmol/L ribavirin. The eGFP signal of each well was analyzed by a high content screening system at 24 hpi (**A**) and 36 hpi (**B**), respectively. For each condition, six wells were performed in parallel. The error bars represent the standard deviations. **C** The Z′ value of each condition calculated from the SFV-eGFP infected cells treated and untreated with ribavirin.

Assays amenable to HTS of antiviral compounds from large drug libraries can facilitate the drug discovery process. For highly pathogenic viruses, several HTS-based antiviral assays that can overcome the limitation of the need for high-level biosafety containment have been developed. Viral proteins that have enzymatic activities usually play essential roles in viral replication, and are attractive targets for antiviral agents. By designing *in vitro* biochemical reactions with purified enzymes and proper substrates, the enzymatic activities can be measured in a high-throughput manner. The enzyme target-based HTS antiviral assays have been established in several viruses such as influenza viruses (Su et al., 2010), flaviviruses (Johnston et al., 2007; Manzano et al., 2014) and SARS-CoV-2 (Rothan and Teoh, 2021; Bai et al., 2022). For alphaviruses,

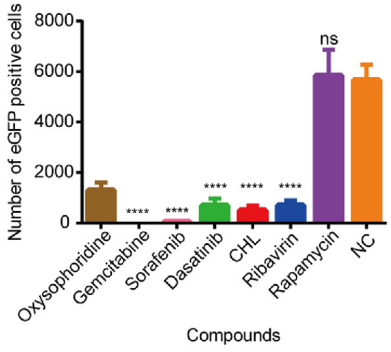

Fig. 7. Validation of the availability of SFV-eGFP HTS assay for screening broad spectrum antiviral against alphaviruses using reference inhibitors. BHK-21 cells were seeded in 96-well plates and infected with SFV-eGFP at an MOI of 1, and then treated with 5 μmol/L oxysophoridine, 5 μmol/L gemcitabine, 5 μmol/L sorafenib, 10 μmol/L dasatinib, 5 μmol/L CHL, and 41 μmol/L ribavirin, respectively. The rapamycin (1 μmol/L) and 1% DMSO (NC) were used as negative controls. At 24 hpi, the fluorescence value of the cells was read by a high content screening system. For each drug, six wells were performed in parallel. Error bars indicate the standard deviations. The differences between each compound and DMSO were analyzed using one-way ANOVA. ****$P <$ 0.0001; ns, not significant.

the nsP1 capping enzyme, nsP2 protease and capsid protease-targeted HTS assay have been developed to screen CHIKV inhibitors (Aggarwal et al., 2015; Bullard-Feibelman et al., 2016; Saha et al., 2018). Using reverse genetics system of RNA viruses, the replicons which lack viral structural genes, and the propagation-defective pseudovirus particles coating heterologous or homologous viral envelop proteins can be generated, and provide safe tools to screen inhibitors targeting viral replication and entry process respectively. The replicon-based or pseudovirus-based HTS antiviral assays have been established for a number of viral species, including coronaviruses, flaviviruses and enteroviruses (Fernandes et al., 2020; Xiang et al., 2022). These target-, replicon-, and pseudovirus-based HTS assays enable safe handling under BSL-2 conditions. However, these methods screen on specific stages during viral life cycle, lowering the number of total potential hits as compared to the authentic virus-based HTS assay which screen inhibitors targeting to the entire viral life cycle. Viruses that are classified in the same genus have similar genome structure and exhibit high conservation of the viral protein function, which represent potential broad-spectrum targets of the viral genus. Therefore, the viruses that have lower biosafety risks are capable to serve as safe substitutes for BSL-3/4 pathogens belonging to the same genus to develop the live virus-based HTS assay. For instances, the nonpathogenic *Henipavirus*, Cedar virus-based HTS assay was developed for antiviral discovery of the highly pathogenic Nipah virus and Hendra virus (Amaya et al., 2021), and recombinant human coronavirus OC43 (HCoV-OC43) reporter virus was adapted to a HTS platform to search for effective inhibitors to the highly pathogenic SARS-CoV and MERS-CoV (Shen et al., 2019). Here, using a panel of known inhibitors against CHIKV and VEEV in reference and our unpublished work, we validated that the compounds, showing antiviral effects on these highly pathogenic alphaviruses, also efficiently inhibited SFV-eGFP virus. Therefore, the SFV-eGFP virus-based HTS assay which combines the advantages of broader target base and lower biosafety limitation, provides a safe platform to screen potential broad-spectrum inhibitors of highly pathogenic alphaviruses in BSL-2 facilities.

Generally, the authentic virus-based HTS assays were developed using recombinant reporter viruses. For the choice of reporter genes, with

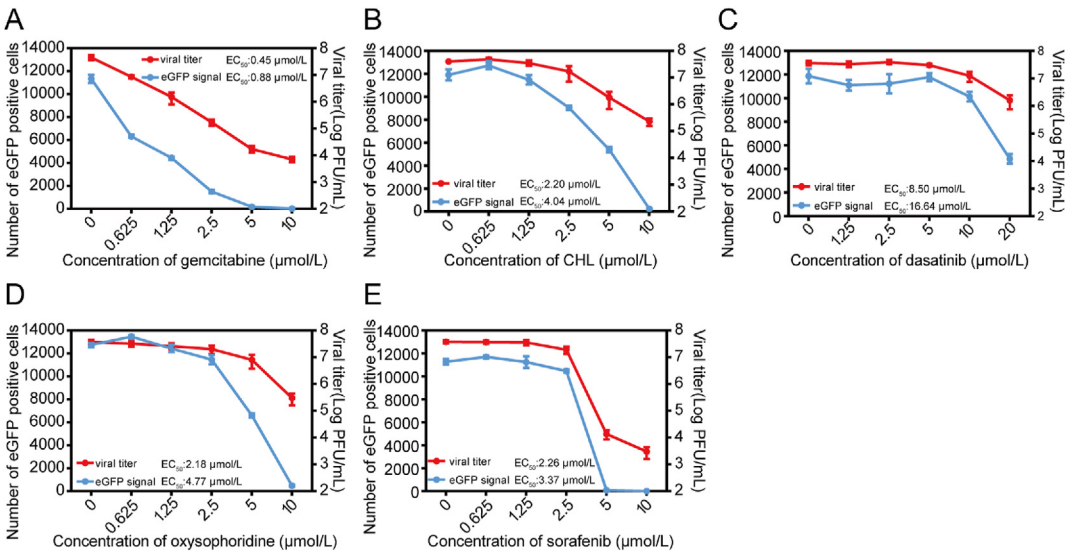

Fig. 8. Detection of EC_{50} of the reference inhibitors by SFV-eGFP based HTS assay and plaque assay. BHK-21 cells were seeded in 96-well plates and infected with SFV-eGFP at an MOI of 1, and then treated with 0, 0.625, 1.25, 2.5, 5, and 10 μmol/L gemcitabin (**A**), CHL (**B**), oxysophoridine (**D**), and sorafenib (**E**) and 0, 1.25, 2.5, 5, 10, and 20 μmol/L dasatinib (**C**), respectively. At 24 hpi, the fluorescence value of the cells was read by a high content screening system. Meanwhile, the supernatants of the cells were collected at 24 hpi and subjected to plaque assay to determine the viral titers. Error bars indicate the standard deviations from three independent experiments. The EC_{50} value of each compound was calculated by viral titers and eGFP signals, respectively, using GraphPad Prism software.

the development of image-based HCS technology, the fluorescent proteins can be visually and quantitatively detected, providing ideal choice for the reporter virus-based HTS antiviral assay. However, since the inserted reporter gene is not required for viral replication, it will inevitably be excluded after extensive virus passage, leading to diminished expression of the reporter protein in the reporter virus infected cells. Therefore, the instability of the reporter gene poses a common challenge for the utilization of reporter viruses. The genetic stability of reporter gene is influenced by the gene type and size, the culture cell type, as well as the strategy to insert into viral genome. We had previously constructed the eGFP labeled CHIKV (CHIKV-eGFP) and MAYV (MAYV-eGFP) respectively by introducing an additional subgenomic promoter to express the *eGFP* gene between the 5′ORF and 3′ORF in the genome. Both CHIKV-eGFP and MAYV-eGFP exhibited similar replication kinetics with their wild type viruses and can be stably maintained for at least five rounds of passage in BHK-21 cells (Deng et al., 2016; Li et al., 2019). However, the replication of SFV-eGFP generated using the same strategy was delayed compared with the wild type SFV, and the eGFP started to loss significantly from passage 4 (Fig. 4). We supposed that the accelerated eGFP loss of SFV-eGFP may be due to its lower replication than that of wild type SFV, placing it at a competitive disadvantage during passage. Furthermore, we found that SFV-eGFP exhibited preferable stability in BHK-21 cells than that in Vero and Huh7 cells (Fig. 3), possibly due to different replication kinetics of SFV-eGFP in different cell types. Therefore, for the use of SFV-eGFP, it is better to prepare virus stocks in BHK-21 cells within three or less passages to insure the maintenance of reporter gene.

5. Conclusions

A recombinant SFV-eGFP virus with high-titer production and favorable genetic stability was generated for use in image-based HTS antiviral assays using HCS system. This SFV-eGFP based HTS assay provides a safe and convenient platform for screening broad-spectrum drugs against alphaviruses, which will contribute to the control of highly pathogenic alphaviruses.

Data availability

All data supporting the findings of this study are available within the article or from the corresponding author upon reasonable request.

Ethics statement

This article does not contain any studies with human or animal subjects performed by any of the authors.

Author contributions

Yu-Jia Shi: data curation; Jia-Qi Li: visualization, investigation; Hong-Qing Zhang: visualization, investigation; Cheng-Lin Deng: visualization, investigation; Qin-Xuan Zhu: visualization, investigation; Bo Zhang: conceptualization, methodology; Xiao-Dan Li: conceptualization, methodology.

Conflict of interest

Prof. Bo Zhang is an Editorial Board member for *Virologica Sinica* and was not involved in the editorial review or the decision to publish this article. All authors declare that they have no conflict of interest.

Acknowledgements

This work was supported by the Creative Research Group Program of Natural Science Foundation of Hubei Province (2022CFA021) and National Natural Science Foundation of China (81702005). The funders had no role in study design, data collection and interpretation, or the decision to submit the work for publication.

Appendix A. Supplementary data

Supplementary data to this article can be found online at https://doi.org/10.1016/j.virs.2023.06.007.

References

Aggarwal, M., Sharma, R., Kumar, P., Parida, M., Tomar, S., 2015. Kinetic characterization of trans-proteolytic activity of Chikungunya virus capsid protease and development of a FRET-based HTS assay. Sci. Rep. 5, 14753.

Amarilla, A.A., Sng, J.D.J., Parry, R., Deerain, J.M., Potter, J.R., Setoh, Y.X., Rawle, D.J., Le, T.T., Modhiran, N., Wang, X., Peng, N.Y.G., Torres, F.J., Pyke, A., Harrison, J.J., Freney, M.E., Liang, B., McMillan, C.L.D., Cheung, S.T.M., Guevara, D., Hardy, J.M., Bettington, M., Muller, D.A., Coulibaly, F., Moore, F., Hall, R.A., Young, P.R., Mackenzie, J.M., Hobson-Peters, J., Suhrbier, A., Watterson, D., Khromykh, A.A., 2021. A versatile reverse genetics platform for SARS-CoV-2 and other positive-strand RNA viruses. Nat. Commun. 12, 3431.

Amaya, M., Cheng, H., Borisevich, V., Navaratnarajah, C.K., Cattaneo, R., Cooper, L., Moore, T.W., Gaisina, I.N., Geisbert, T.W., Rong, L., Broder, C.C., 2021. A recombinant Cedar virus based high-throughput screening assay for henipavirus antiviral discovery. Antiviral Res. 193, 105084.

Azar, S.R., Campos, R.K., Bergren, N.A., Camargos, V.N., Rossi, S.L., 2020. Epidemic alphaviruses: ecology, emergence and outbreaks. Microorganisms 8, 1167.

Bai, X., Sun, H., Wu, S., Li, Y., Wang, L., Hong, B., 2022. Identifying small-molecule inhibitors of SARS-CoV-2 RNA-dependent RNA polymerase by establishing a fluorometric assay. Front. Immunol. 13, 844749.

Briolant, S., Garin, D., Scaramozzino, N., Jouan, A., Crance, J.M., 2004. In vitro inhibition of Chikungunya and Semliki Forest viruses replication by antiviral compounds: synergistic effect of interferon-alpha and ribavirin combination. Antiviral Res. 61, 111–117.

Bullard-Feibelman, K.M., Fuller, B.P., Geiss, B.J., 2016. A sensitive and robust high-throughput screening assay for inhibitors of the Chikungunya virus nsP1 capping enzyme. PLoS One 11, e0158923.

Clark, L.E., Clark, S.A., Lin, C., Liu, J., Coscia, A., Nabel, K.G., Yang, P., Neel, D.V., Lee, H., Brusic, V., Stryapunina, I., Plante, K.S., Ahmed, A.A., Catteruccia, F., Young-Pearse, T.L., Chiu, I.M., Llopis, P.M., Weaver, S.C., Abraham, J., 2022. VLDLR and ApoER2 are receptors for multiple alphaviruses. Nature 602, 475–480.

Creanga, A., Gillespie, R.A., Fisher, B.E., Andrews, S.F., Lederhofer, J., Yap, C., Hatch, L., Stephens, T., Tsybovsky, Y., Crank, M.C., Ledgerwood, J.E., McDermott, A.B., Mascola, J.R., Graham, B.S., Kanekiyo, M., 2021. A comprehensive influenza reporter virus panel for high-throughput deep profiling of neutralizing antibodies. Nat. Commun. 12, 1722.

Deng, C.L., Liu, S.Q., Zhou, D.G., Xu, L.L., Li, X.D., Zhang, P.T., Li, P.H., Ye, H.Q., Wei, H.P., Yuan, Z.M., Qin, C.F., Zhang, B., 2016. Development of neutralization assay using an eGFP Chikungunya virus. Viruses 8, 181.

Fazakerley, J.K., 2002. Pathogenesis of Semliki Forest virus encephalitis. J. Neurovirol. 8 (Suppl. 2), 66–74.

Fernandes, R.S., Freire, M., Bueno, R.V., Godoy, A.S., Gil, L., Oliva, G., 2020. Reporter replicons for antiviral drug discovery against positive single-stranded RNA viruses. Viruses 12, 598.

Huang, Y.H., Huang, J.T., 2021. Use of chlorhexidine to eradicate oropharyngeal SARS-CoV-2 in COVID-19 patients. J. Med. Virol. 93, 4370–4373.

Huffman, J.H., Sidwell, R.W., Khare, G.P., Witkowski, J.T., Allen, L.B., Robins, R.K., 1973. In vitro effect of 1-beta-D-ribofuranosyl-1,2,4-triazole-3-carboxamide (virazole, ICN 1229) on deoxyribonucleic acid and ribonucleic acid viruses. Antimicrob. Agents Chemother. 3, 235–241.

Johnston, P.A., Phillips, J., Shun, T.Y., Shinde, S., Lazo, J.S., Huryn, D.M., Myers, M.C., Ratnikov, B.I., Smith, J.W., Su, Y., Dahl, R., Cosford, N.D., Shiryaev, S.A., Strongin, A.Y., 2007. HTS identifies novel and specific uncompetitive inhibitors of the two-component NS2B-NS3 proteinase of West Nile virus. Assay Drug Dev. Technol. 5, 737–750.

Joubert, P.E., Stapleford, K., Guivel-Benhassine, F., Vignuzzi, M., Schwartz, O., Albert, M.L., 2015. Inhibition of mTORC1 enhances the translation of Chikungunya proteins via the activation of the MnK/eIF4E pathway. PLoS Pathog. 11, e1005091.

Khan, M., Santhosh, S.R., Tiwari, M., Lakshmana Rao, P.V., Parida, M., 2010. Assessment of in vitro prophylactic and therapeutic efficacy of chloroquine against Chikungunya virus in vero cells. J. Med. Virol. 82, 817–824.

Lello, L.S., Utt, A., Bartholomeeusen, K., Wang, S., Rausalu, K., Kendall, C., Coppens, S., Fragkoudis, R., Tuplin, A., Alphey, L., Arien, K.K., Merits, A., 2020. Cross-utilisation of template RNAs by alphavirus replicases. PLoS Pathog. 16, e1008825.

Li, X., Zhang, H., Zhang, Y., Li, J., Wang, Z., Deng, C., Jardim, A.C.G., Terzian, A.C.B., Nogueira, M.L., Zhang, B., 2019. Development of a rapid antiviral screening assay based on eGFP reporter virus of Mayaro virus. Antiviral Res. 168, 82–90.

Liljestrom, P., Lusa, S., Huylebroeck, D., Garoff, H., 1991. In vitro mutagenesis of a full-length cDNA clone of Semliki Forest virus: the small 6,000-molecular-weight membrane protein modulates virus release. J. Virol. 65, 4107–4113.

Lundberg, L., Brahms, A., Hooper, I., Carey, B., Lin, S.C., Dahal, B., Narayanan, A., Kehn-Hall, K., 2018. Repurposed FDA-Approved drug sorafenib reduces replication of Venezuelan equine encephalitis virus and other alphaviruses. Antiviral Res. 157, 57–67.

Lundstrom, K., 2014. Alphavirus-based vaccines. Viruses 6, 2392–2415.

Lundstrom, K., 2020. Semliki Forest virus-based immunotherapy for cancer. Expert Opin. Biol. Ther. 20, 593–599.

Maheshwari, R.K., Husain, M.M., Attallah, A.M., Friedman, R.M., 1983. Tunicamycin treatment inhibits the antiviral activity of interferon in mice. Infect. Immun. 41, 61–66.

Manzano, M., Padia, J., Padmanabhan, R., 2014. Small molecule inhibitor discovery for dengue virus protease using high-throughput screening. Methods Mol. Biol. 1138, 331–344.

Mohankumar, V., Dhanushkodi, N.R., Raju, R., 2011. Sindbis virus replication, is insensitive to rapamycin and torin1, and suppresses Akt/mTOR pathway late during infection in HEK cells. Biochem. Biophys. Res. Commun. 406, 262–267.

Perez, L., Irurzun, A., Carrasco, L., 1993. Activation of phospholipase activity during Semliki Forest virus infection. Virology 194, 28–36.

Pohjala, L., Barai, V., Azhayev, A., Lapinjoki, S., Ahola, T., 2008. A luciferase-based screening method for inhibitors of alphavirus replication applied to nucleoside analogues. Antiviral Res. 78, 215–222.

Reichert, E., Clase, A., Bacetty, A., Larsen, J., 2009. Alphavirus antiviral drug development: scientific gap analysis and prospective research areas. Biosecur. Bioterror. 7, 413–427.

Rothan, H.A., Bahrani, H., Mohamed, Z., Teoh, T.C., Shankar, E.M., Rahman, N.A., Yusof, R., 2015. A combination of doxycycline and ribavirin alleviated chikungunya infection. PLoS One 10, e0126360.

Rothan, H.A., Teoh, T.C., 2021. Cell-based high-throughput screening protocol for discovering antiviral inhibitors against SARS-COV-2 main protease (3CLpro). Mol. Biotechnol. 63, 240–248.

Roy, C.J., Reed, D.S., Hutt, J.A., 2010. Aerobiology and inhalation exposure to biological select agents and toxins. Vet. Pathol. 47, 779–789.

Saha, A., Acharya, B.N., Priya, R., Tripathi, N.K., Shrivastava, A., Rao, M.K., Kesari, P., Narwal, M., Tomar, S., Bhagyawant, S.S., Parida, M., Dash, P.K., 2018. Development of nsP2 protease based cell free high throughput screening assay for evaluation of inhibitors against emerging Chikungunya virus. Sci. Rep. 8, 10831.

Shen, L., Niu, J., Wang, C., Huang, B., Wang, W., Zhu, N., Deng, Y., Wang, H., Ye, F., Cen, S., Tan, W., 2019. High-throughput screening and identification of potent broad-spectrum inhibitors of coronaviruses. J. Virol. 93, e00023-00019.

Shin, G., Yost, S.A., Miller, M.T., Elrod, E.J., Grakoui, A., Marcotrigiano, J., 2012. Structural and functional insights into alphavirus polyprotein processing and pathogenesis. Proc. Natl. Acad. Sci. U. S. A. 109, 16534–16539.

Smee, D.F., Morris, J.L., Barnard, D.L., Van Aerschot, A., 1992. Selective inhibition of arthropod-borne and arenaviruses in vitro by 3'-fluoro-3'-deoxyadenosine. Antiviral Res. 18, 151–162.

Steinberg, M., 2007. Dasatinib: a tyrosine kinase inhibitor for the treatment of chronic myelogenous leukemia and philadelphia chromosome-positive acute lymphoblastic leukemia. Clin. Ther. 29, 2289–2308.

Su, C.Y., Cheng, T.J., Lin, M.I., Wang, S.Y., Huang, W.I., Lin-Chu, S.Y., Chen, Y.H., Wu, C.Y., Lai, M.M., Cheng, W.C., Wu, Y.T., Tsai, M.D., Cheng, Y.S., Wong, C.H., 2010. High-throughput identification of compounds targeting influenza RNA-dependent RNA polymerase activity. Proc. Natl. Acad. Sci. U. S. A. 107, 19151–19156.

Tamberg, N., Lulla, V., Fragkoudis, R., Lulla, A., Fazakerley, J.K., Merits, A., 2007. Insertion of EGFP into the replicase gene of Semliki Forest virus results in a novel, genetically stable marker virus. J. Gen. Virol. 88, 1225–1230.

Tarbatt, C.J., Glasgow, G.M., Mooney, D.A., Sheahan, B.J., Atkins, G.J., 1997. Sequence analysis of the avirulent, demyelinating A7 strain of Semliki Forest virus. J. Gen. Virol. 78 (Pt 7), 1551–1557.

Teppor, M., Zusinaite, E., Karo-Astover, L., Omler, A., Rausalu, K., Lulla, V., Lulla, A., Merits, A., 2021. Semliki Forest virus chimeras with functional replicase modules from related alphaviruses survive by adaptive mutations in functionally important hot spots. J. Virol. 95, e0097321.

Van Aerschot, A., Herdewijn, P., Janssen, G., Cools, M., De Clercq, E., 1989. Synthesis and antiviral activity evaluation of 3'-fluoro-3'-deoxyribonucleosides: broad-spectrum antiviral activity of 3'-fluoro-3'-deoxyadenosine. Antiviral Res. 12, 133–150.

Weisshaar, M., Cox, R., Morehouse, Z., Kumar Kyasa, S., Yan, D., Oberacker, P., Mao, S., Golden, J.E., Lowen, A.C., Natchus, M.G., Plemper, R.K., 2016. Identification and characterization of influenza virus entry inhibitors through dual myxovirus high-throughput screening. J. Virol. 90, 7368–7387.

Xiang, Q., Li, L., Wu, J., Tian, M., Fu, Y., 2022. Application of pseudovirus system in the development of vaccine, antiviral-drugs, and neutralizing antibodies. Microbiol. Res. 258, 126993.

Xie, X., Muruato, A., Lokugamage, K.G., Narayanan, K., Zhang, X., Zou, J., Liu, J., Schindewolf, C., Bopp, N.E., Aguilar, P.V., Plante, K.S., Weaver, S.C., Makino, S., LeDuc, J.W., Menachery, V.D., Shi, P.Y., 2020. An infectious cDNA clone of SARS-CoV-2. Cell Host Microbe 27, 841–848.e3.

Zhang, J.H., Chung, T.D., Oldenburg, K.R., 1999. A simple statistical parameter for use in evaluation and validation of high throughput screening assays. J. Biomol. Screen. 4, 67–73.

Zhang, J.W., Wang, H., Liu, J., Ma, L., Hua, R.H., Bu, Z.G., 2021. Generation of a stable GFP-reporter Zika virus system for high-throughput screening of Zika virus inhibitors. Virol. Sin. 36, 476–489.

Zhang, Y.N., Zhang, Q.Y., Li, X.D., Xiong, J., Xiao, S.Q., Wang, Z., Zhang, Z.R., Deng, C.L., Yang, X.L., Wei, H.P., Yuan, Z.M., Ye, H.Q., Zhang, B., 2020. Gemcitabine, lycorine and oxysophoridine inhibit novel coronavirus (SARS-CoV-2) in cell culture. Emerg. Microbes Infect. 9, 1170–1173.

Zhang, Z.R., Zhang, H.Q., Li, X.D., Deng, C.L., Wang, Z., Li, J.Q., Li, N., Zhang, Q.Y., Zhang, H.L., Zhang, B., Ye, H.Q., 2020a. Generation and characterization of Japanese encephalitis virus expressing GFP reporter gene for high throughput drug screening. Antiviral Res. 182, 104884.

Zhang, Z.R., Zhang, Y.N., Li, X.D., Zhang, H.Q., Xiao, S.Q., Deng, F., Yuan, Z.M., Ye, H.Q., Zhang, B., 2020b. A cell-based large-scale screening of natural compounds for inhibitors of SARS-CoV-2. Signal Transduct. Target. Ther. 5, 218.

Zou, G., Xu, H.Y., Qing, M., Wang, Q.Y., Shi, P.Y., 2011. Development and characterization of a stable luciferase dengue virus for high-throughput screening. Antiviral Res. 91, 11–19.